J Solid State Electrochem (2007) 11:1421–1427
DOI 10.1007/s10008-007-0300-x

ORIGINAL PAPER

The effects of a eutectic modifier on microstructure and surface corrosion behavior of Al-Si hypoeutectic alloys

Wislei R. Osório · Noé Cheung · José E. Spinelli · Pedro R. Goulart · Amauri Garcia

Received: 5 January 2007 / Revised: 27 February 2007 / Accepted: 7 March 2007 / Published online: 29 March 2007
© Springer-Verlag 2007

Abstract Hypoeutectic aluminum–silicon alloys can have significant improvements in mechanical properties by inducing structural modification in the normally occurring eutectic. The eutectic modification may affect not only the mechanical properties but also the corrosion resistance of such alloys. It is well known that structural parameters such as grain size and interdendritic spacing can significantly affect corrosion resistance of alloys. However, to date, few researches have been performed to experimentally evaluate the effects of an effective modification of eutectic morphology on surface corrosion behavior of Al–Si alloys. In the present study, modified and unmodified samples of an Al 9 wt.% Si alloy were solidified under similar solidification conditions, and after metallographic procedures, the corrosion resistance was analyzed by both the electrochemical impedance spectroscopy technique and the Tafel extrapolation method carried out in a 0.5 M NaCl test solution at 25 °C. The impedance parameters and corrosion rate were obtained from an equivalent circuit analysis. It was found that the Al-9 wt.% Si alloy casting in the modified condition tends to have its corrosion resistance decreased when compared to the unmodified alloy.

Keywords Corrosion resistance · Eutectic modification · Electrochemical behavior · Al–Si hypoeutectic alloys

W. R. Osório · N. Cheung · J. E. Spinelli · P. R. Goulart · A. Garcia (✉)
Department of Materials Engineering,
State University of Campinas (UNICAMP),
P.O. Box 6122, 13083-970 Campinas, SP, Brazil
e-mail: amaurig@fem.unicamp.br

Introduction

Aluminum alloys with silicon as a major alloying element constitute a class of material, which provides the most significant part of all shaped castings manufactured, have wide-ranging applications in the automotive and aerospace industries [1]. This is mainly because of the outstanding effect of silicon in the improvement of casting characteristics such as a high degree of fluidity in the molten condition and a very low tendency to the development of unsoundness, combined with other physical properties such as mechanical properties and corrosion resistance. These alloys form a simple eutectic system between elementary silicon and aluminum, the eutectic point occurring at about 12% silicon. In general, an optimum range of silicon content can be assigned to casting processes. For slow-cooling rate processes (sand, plaster, investment) the range is 5–7 wt.%, for permanent molds 7–9% and for die castings 8–12% [2].

A maximum of 1.6% silicon can dissolve in the aluminum with the limit decreasing to less than a tenth of this value at temperatures below 300 °C. The typical hypoeutectic aluminum–silicon alloys have two major microstructural components namely, primary aluminum and an aluminum–silicon eutectic. For metal-non-metal eutectics, the growth form of the faceting phase is such as to produce a three-dimensional skeletal crystal rather than thin sheets. Although the silicon plates appear to be separate crystals, they are in fact interconnected. Mechanical properties of Al–Si casting alloys depend not only on their chemical composition but are also significantly dependent on microstructural features such as the morphologies of the Al-rich α-phase and of the eutectic Si particles. Eutectic Si in untreated Al–Si foundry alloys often has a very coarse and plate-like morphology, leading to poor

mechanical properties, particularly ductility [3]. Significant improvement in mechanical properties can be achieved when the Al–Si alloys undergo a change in the morphological characteristics of silicon both in eutectic and primary form by modification, with certain additions made to the molten alloy, e.g., antimony, strontium, sodium and titanium [4–8]. Particularly, the addition of sodium causes the disappearance of primary silicon with the formation of solid solution dendrites (α-Al) and fine fiber eutectic silicon instead of plate-like structures [5], resulting in a highly branched filamentary form with a better distribution of Si particles.

The effect of microstructure on metallic alloys properties has been highlighted in various studies and particularly, the influence of dendrite arm spacing upon the mechanical properties, i.e., ultimate tensile strength, yield strength, and tensile elongation, has been reported [9–17]. In the as-cast state, an alloy may possess within individual grains a dendritic network of continuously varying solute content, second phases, and possibly porosity and inclusions (as shown schematically in Fig. 1), which have a significant influence on final properties [12].

Although the use of modifiers in Al–Si alloys promotes an improvement on mechanical properties, studies are still needed to clarify the influence of modifiers on the corrosion resistance. It is well known that structural parameters such as grain size and interdendritic spacing strongly affect corrosion resistance of as-cast alloys [18–20]. For a hypoeutectic Zn4Al alloys, it was found that the structural dendritic refinement provides both higher corrosion resistance and better mechanical properties [20]. A recent study has shown that such result cannot be considered as a general trend because the dendritic refinement has improved the tensile strength of both a Zn-27Al (hypereutectic) and an Al9 wt.% Si (hypoeutectic) alloys, however coupled with a reduction on the corrosion resistance [21].

There is a lack of consistent studies and experimental reports on the effect of an effective modification of the eutectic silicon morphology on surface corrosion behavior of Al–Si alloys. The present study aims to contribute to the understanding of the role of the structural refinement brought about by modification on the corrosion resistance. Modified and unmodified Al 9 wt.% Si samples were cast under similar operational conditions to parameterize the cooling rates along solidification. After metallographic procedures and microscopy analysis, the corrosion resistance was evaluated by both the electrochemical impedance spectroscopy (EIS) technique and the Tafel extrapolation method carried out in a 0.5 M NaCl test solution at 25 °C. The impedance parameters were obtained from an equivalent circuit.

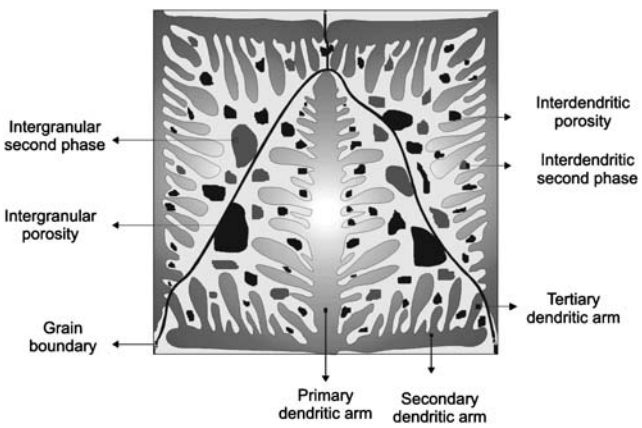

Fig. 1 Schematic representation of a typical as-cast microstructure

Experimental procedure

Modified and unmodified Al-9 wt.% Si alloy samples were used in the experiments. The alloy was prepared from commercially pure materials, whose chemical compositions are presented in Table 1.

The alloy was prepared in a silicon carbide crucible and was melted in an electric resistance-type furnace until the molten metal reached a predetermined temperature to perform a thermal analysis for calibrating its silicon content. A metallic mold made of carbon steel was used in the experiments to obtain the modified and unmodified samples of Al-9 wt.% Si alloy. The carbon steel mold has an internal diameter of 44 mm, height of 10 mm, 10-mm wall thickness, and 6-mm bottom thickness.

Before being poured into the mold cavity, the alloy was stirred until the temperature was brought to 675 °C (70 °C above the *liquidus* temperature). Besides, the alloy was degassed by injecting argon gas into the melt during at least 5 min before pouring. A type K thermocouple, sheathed in a stainless steel protection tube having an outside diameter of 1.6 mm, was used to measure the melt temperature immediately before pouring the alloy into the mold cavity. A data logger that was connected to a computer was used to monitor the temperature. The same degree of superheat was maintained for both experiments.

In the case of the modified alloy condition, before the degassing procedure, the modifier was sprinkled against the

Table 1 Chemical composition of materials used to prepare the Al–Si alloy

Chemical composition (wt.%)					
Element	P	Fe	Si	Zn	Mn
Al	*	0.092	0.180	0.007	*
Si	0.010	0.216	*	*	*

*Less than 50 ppm.

liquid-metal surface. Then, the melt was stirred to incorporate this modifier into the liquid, which was allowed to remain in contact with the melt for approximately 8 min. The used sodium modifier was a commercial flux (Modimil^R), which contains mainly sodium fluoride. According to the literature [6, 22], 1% of the melt weight of Modimil^R flux is enough to achieve the eutectic modification.

Both samples were carefully solidified under similar cooling conditions. The corresponding microstructures were revealed through grinding, polishing, and etching selected regions of the samples. The chemical etchant used was a solution of 0.5% HF in distilled water. Image processing systems Neophot 32 (Carl Zeiss, Esslingen, Germany) and Leica Quantimet 500 MC (Leica Imaging Systems, Cambridge, England) were used to acquire the microstructures. Secondary dendrite arm spacings (λ_2) were measured by averaging the distance between adjacent side branches.

EIS and polarization tests were carried out in triplicate for both modified and unmodified samples. The EIS tests were carried out in a 0.5-M NaCl solution at 25 °C and a neutral pH range (6.5). A potentiostat coupled to a frequency analyzer system, a glass corrosion cell kit with a platinum counter electrode, and a saturated calomel reference electrode (SCE) were used to perform the EIS test. The working electrodes consisted of as-cast alloy samples, which were positioned at the glass corrosion cell kit, leaving a circular 1-cm^2 metal surface in contact with the electrolyte. The potential amplitude was set to 10 mV in open-circuit potential, and the frequency range was set from 100 mHz to 100 kHz. The samples were further ground to a 600-grit SiC finish, followed by distilled water washing and air drying before measurements. EIS measurements began after an initial delay of 10 min for the sample to reach a steady-state condition.

Polarization tests were also carried out in a 0.5-M NaCl solution at 25 °C using a potentiostat. The polarization curves were determined by stepping the potential at a scan rate of 0.2 mV/s, from −250 mV (SCE) to +250 mV (SCE) related to open-circuit potential. Using an automatic data acquisition system, the potentiodynamic polarization curves were plotted, and both corrosion rate and potential were estimated by the Tafel extrapolation method.

Results and discussion

The resulting macrostructures for both unmodified and modified Al-9 wt.% Si as-cast samples are shown in Fig. 2. Observing such macrographies, it can be noticed that a similar average grain size (GS) was obtained for both cases, of about 5 mm in diameter, as indicated in Fig. 2. Such similarity can be attributed to the similar conditions

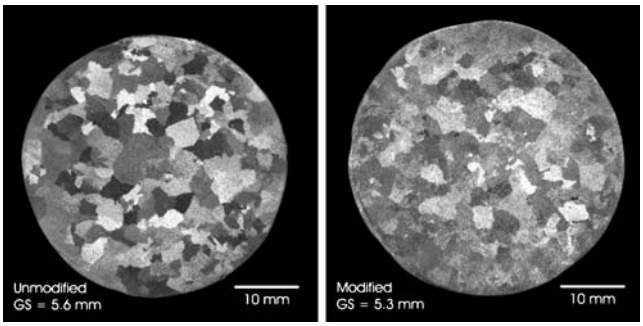

Fig. 2 Macrostructures for unmodified and modified Al 9 wt.% Si as-cast samples and corresponding GS

provided by the experimental procedures for both samples. This is expected as the modifier is used basically to change the morphology of the eutectic Si. Indeed, the eutectic modifier does not affect the nucleation rate in the first stages of solidification and, consequently, the final grain sizes are similar for both modified and unmodified samples.

Figure 3 shows the microstructures obtained by optical microscopy for unmodified and modified Al-9 wt.% Si-casting samples. By analyzing the sample in which sodium-modifier was added to the melt, a considerable eutectic modification can be observed. Its microstructural features result in fine and fibrous eutectic silicon, as shown in Fig. 3b. The addition of a modifier has provoked a significant eutectic modification, while the mean GS, the observed dendrite arm spacings (λ_2), and the Al-rich dendritic matrix appear to be unaffected, as expected. On the other hand, the unmodified casting sample has a microstructure characterized by an Al-rich dendritic matrix (α-Al phase) and the eutectic Si particles, which are coarse and distributed in a plate-like morphology, as shown in Fig. 3a.

Figure 4 shows a comparison of experimental results of corrosion tests carried out in a 0.5-M NaCl solution concerning EIS diagrams and potentiodynamic polarization curves for modified and unmodified Al-9 wt.% Si alloy samples, respectively. Qualitative and quantitative analysis from the EIS diagrams, i.e., impedance parameters (polarization resistance and capacitance values), current density, and corrosion potential (obtained from potentiodynamic polarization curves), permit to observe that both the modulus of impedance and the phase angle for the modified alloy sample are lower than those observed for the unmodified alloy, as shown in Fig. 4a. It is well known that higher modulus of impedance and phase angle are conducive to nobler electrochemical behavior [18–20].

Figure 4b shows potentiodynamic polarization curves, and a comparison between the modified and unmodified Al-9 wt.% Si alloy samples can be made. It can be observed that there is a current density about three times higher for the modified sample (of about 3.43 μA/cm^2) compared to

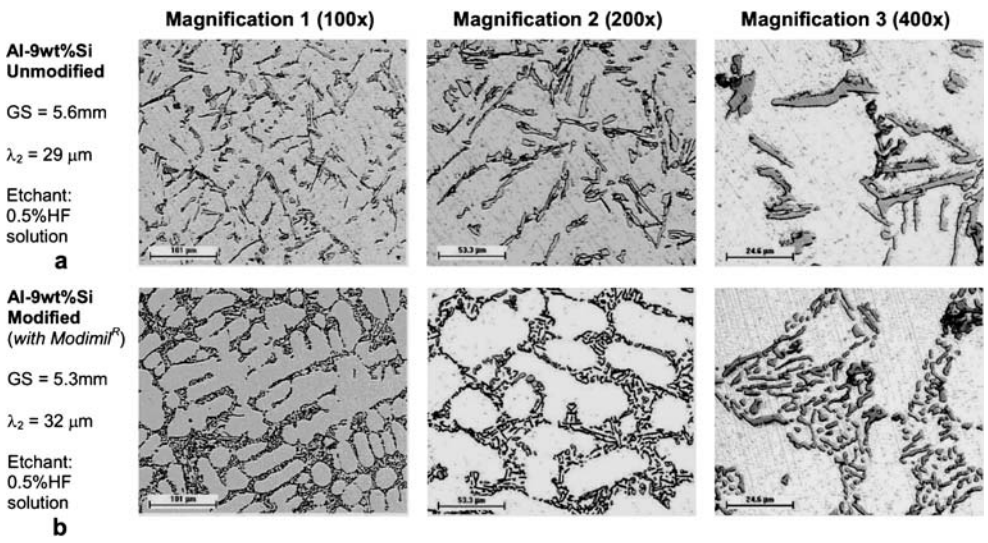

Fig. 3 Microstructures for unmodified and modified Al-9 wt.% Si casting samples and correspondent mean GS

that of the unmodified sample (0.98 μA/cm^2). The modified sample has also presented a corrosion potential slightly more active (or less noble) than the unmodified one. These results provide sufficient information to conclude that the use of the sodium-based modifier had a deleterious effect upon the corrosion behavior of such hypoeutectic Al–Si alloy. However, impedance parameters can provide quantitative and additional information about such tendency.

To supply quantitative support for discussions of these experimental EIS results, an appropriate model (ZView version 2.1b) for equivalent circuit quantification has also been used. The fitting quality was evaluated by chi-squared (χ^2) [23] values, which were interpreted by the ZView software, as shown in Table 2. The chi-squared value is the square of the standard deviation between the original data and the calculated spectrum. It represents an evaluation of the goodness of fit. The electronic equivalent circuit consists of a capacitance component ($Z_{\mathrm{CPE\ 1}}$) in parallel to series resistors R_1 and R_2 and other capacitance component ($Z_{\mathrm{CPE\ 2}}$) in parallel to R_2. The impedance parameter of the equivalent circuit R_{el} corresponds to the electrolyte resistance, which in Bode plot is expressed in a high frequency limit (F>1 kHz). It is proposed that R_1 and the R_2 correspond to the polarization resistance of the samples (modified and unmodified alloy) and oxide film, respectively. These two parameters represent the sum of existing resistances in low frequency limit (F<1 Hz). The parameters n_1 and n_2 are correlated to the phase angle, varying between −1 and 1.The $Z_{\mathrm{CPE(1)}}$ and $Z_{\mathrm{CPE(2)}}$ correspond to the capacitances (1 Hz<F<1 kHz) of the studied samples and its oxide layer formation, respectively. In the literature, Z_{CPE} generally denotes the impedance of a phase element as

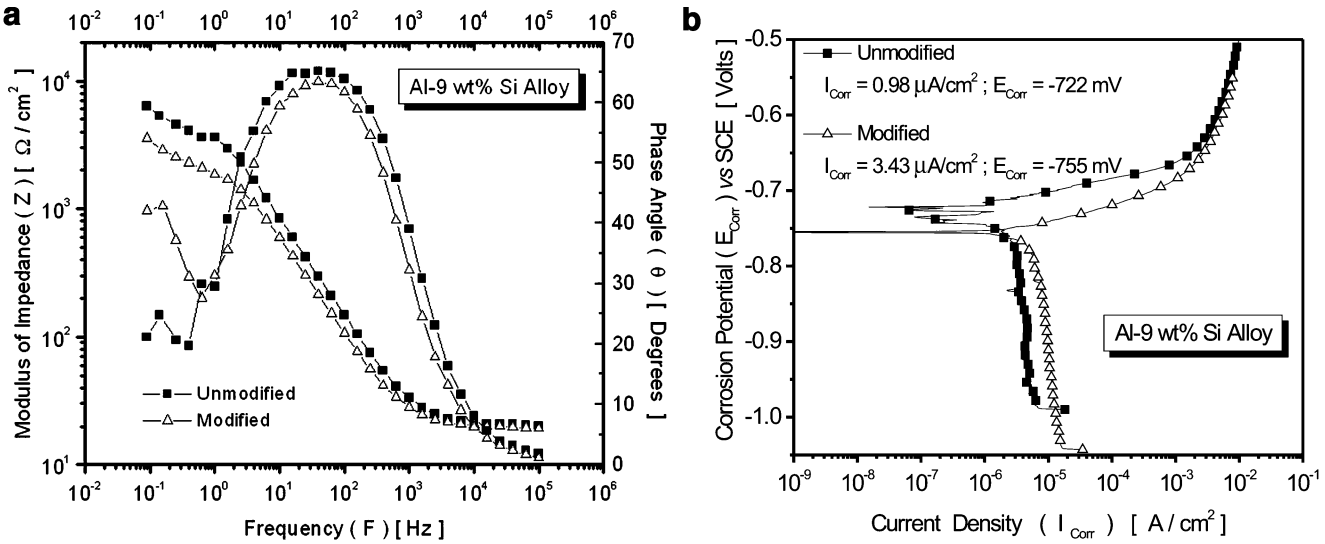

Fig. 4 Experimental results for unmodified and modified Al 9 wt.% Si alloy samples in: **a** EIS tests (Bode and Bode-phase diagrams) and **b** potentiodynamic polarization curves

Table 2 Impedance parameters for the Al-9 wt.% Si alloy samples with unmodified and modified eutectic morphologies in a 0.5-M NaCl test solution

Parameters	Unmodified	Modified
R_{el} (Ω cm^{-2})	20.13	19.39
$Z_{CPE\ (1)}$ ($10^6/\Omega^{-1}$ s^n cm^{-2})	40.56±2.8	50.71±3.1
$Z_{CPE\ (2)}$ ($10^6/\Omega^{-1}$ s^n cm^{-2})	835.17±5.3	547.58±45.4
n_1	0.80	0.82
n_2	0.75	0.85
R_1 (Ω cm^{-2})	5280	2380
R_2 (Ω cm^{-2})	2 10^{15}	2 10^{15}
χ^2	56 10^{-4}	23 10^{-4}

$Z_{CPE}=[C(j\ \omega)^n]^{-1}$,where C is the reciprocal capacitance value, $j=\sqrt{-1}$, ω is the frequency, and n is a parameter varying between 0 and 1 [24, 25].

Figure 5 shows the experimental and simulated curves and the proposed equivalent circuit to fit the experimental data and the corresponding values obtained [23] from the ZView software for the unmodified and modified Al-9 wt.% Si as-cast alloy samples. The impedance parameters shown in Table 2 can confirm the observations concerning the previous qualitative analysis of experimental EIS results, based on Fig. 4a. It can be seen that the unmodified Al-9 wt.% Si-casting sample presents a capacitance $Z_{CPE\ (1)}$ of about 40 $10^6/\Omega^{-1}$ s^n cm^{-2} (or 40 μF cm^{-2}) and a polarization resistance R_1 of about 5280 Ω cm^{-2}. On the other hand, the modified Al-9 wt.% Si cast sample presents a higher capacitance and a lower polarization resistance than the unmodified sample, as shown in Table 2.

The present results give indications that the modified alloy sample is more susceptible to corrosion action in a 0.5-M NaCl solution because of the decrease in R_1 associated with an increase in capacitance, which is conducive to a deleterious effect upon the corrosion behavior. Such tendency of reduction on corrosion resistance presented by the modified alloy sample seems to be associated with an increase in boundaries (between the Al-rich [α] phase and Si particles during growth from the melt) when compared with the unmodified alloy, as the boundaries have proved to be more susceptible to the corrosion action, as previously reported [18, 19, 26].

For hypoeutectic Al–Si alloys, the Al-rich dendritic matrix is delimited by interdendritic regions, which are constituted by a eutectic mixture, i.e., Al-rich phase and Si particles, as can be seen in Fig. 3. However, in both unmodified and modified as-cast samples, the eutectic morphology cannot be considered lamellar but rather, it is formed by Si particles disseminated throughout the Al-rich phase. From the electrochemical point of view, Si is nobler than Al, so that the latter will be more susceptible to corrosion when immersed in some aggressive environment. There are evidences, both theoretical and experimental, suggesting strongly that the interface between a crystal and its melt may be faceted or rough according to the characteristics of the material and the crystallographic nature of the surface. Si is inside the group of materials, which grow from their own melt with surfaces that are faceted and crystallographically significant. On the other hand, metals such as Al normally solidify with surfaces that are not purely crystallographic but are controlled at least in

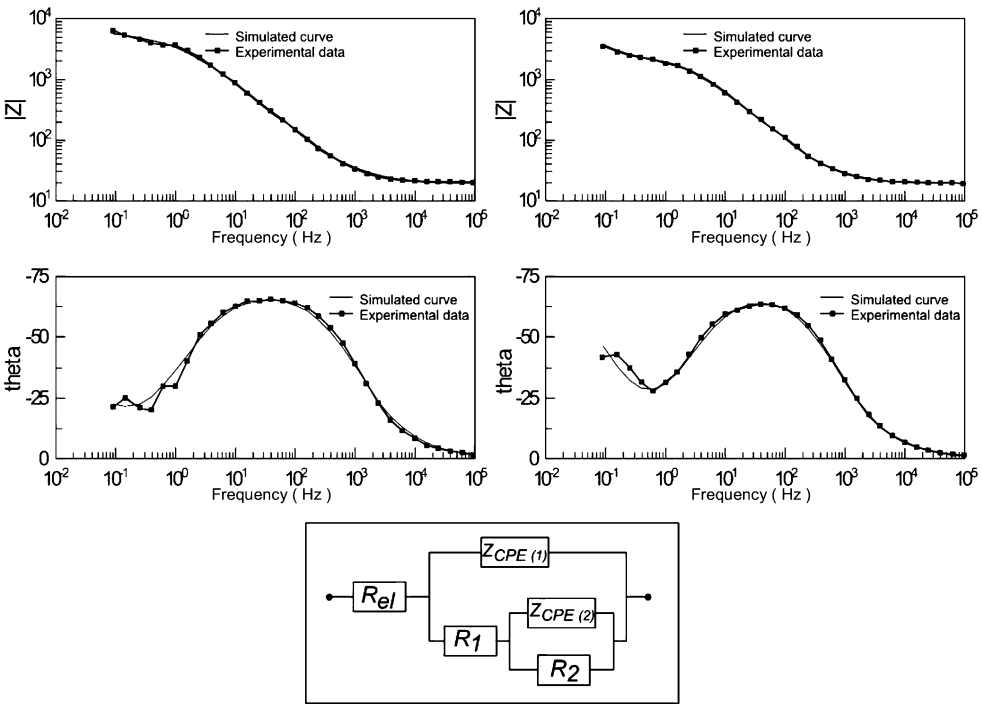

Fig. 5 Experimental and simulated curves obtained by the ZView software for both Al-9 wt.% Si as-cast alloy samples and the proposed equivalent circuit

part by local thermal conditions, and the resulting solid/liquid interface is rough [27]. As a function of such different mentioned growth mechanisms of each phase, its boundaries will not be perfectly conformed but rather will be submitted to a certain deformation at the atomic level, mainly on the α-phase side of the interface. It seems that these regions, because of such localized deformation, are more susceptible to the corrosion action. Although modified and unmodified as-cast samples present similar dendritic spacings (as they were solidified under similar cooling rates) and the same eutectic fraction, the modified sample presents larger localized deformation areas between the Al-rich (α) phase and Si particles because modification induces a morphology typified by highly branched fine silicon fibers and thus contributing to an increase in α/Si surface boundaries. Such increase in areas where corrosion could be initiated and developed will decrease the general corrosion resistance of the modified sample compared with the unmodified condition.

Concerning the impedance parameter R_2, it can be observed that both unmodified and modified alloys present high polarization resistances, which are correlated to the oxide layer formation. In both cases, it can be assumed that a similar mechanism should be responsible by the oxide layer formation because similar R_2 values were found (of about 2 10^{15} Ω cm^{-2}).

The present experimental results provided by EIS diagrams and potentiodynamic polarization curves as well as the fitted equivalent circuit impedance parameters have provided important information concerning the role of the eutectic modifier upon the corrosion behavior of an Al-9 wt.% Si-casting alloy. Thus, such analysis and discussion can be used by the foundry industries to achieve a more reliable quality control of as-cast hypoeutectic Al–Si alloys. Although the addition of eutectic modifiers to Al–Si alloys is widely applied by major foundry industries as an alternative way to produce components with better mechanical properties, the corrosion resistance can be significantly affected, as above discussed. It seems that when a compromise between good corrosion resistance and good mechanical properties is essential, an adequate surface treatment could be provided to improve the surface corrosion resistance of modified Al–Si alloys.

Conclusions

The following main conclusions can be drawn from the present experimental investigation:

1. It is noted that for the decisive characterization of materials, from the point of view of corrosion resistance, other tests are necessary as well besides the EIS and polarization plots. The experimental EIS diagrams, potentiodynamic polarization curves, and fitted equivalent circuit parameters have shown that a modified Al-9 wt.% Si as-cast alloy tends to have its corrosion resistance decreased when compared to the unmodified alloy. Such tendency of reduction on corrosion resistance seems to be associated with the increase in boundaries between the Al-rich (α) phase and Si particles in the modified condition, as the boundaries are more susceptible to the corrosion action. Modification induces a morphology typified by highly branched fine silicon fibers and thus contributing to an increase in α/Si surface boundaries
2. Although eutectic modifiers are widely applied by major foundry industries to attain better mechanical properties in Al-Si alloys castings, care should be taken with the resulting corrosion properties, especially when a good surface corrosion behavior is required.

Acknowledgements The authors acknowledge financial support provided by FAPESP (The Scientific Research Foundation of the State of São Paulo, Brazil), FAEPEX–UNICAMP and CNPq (The Brazilian Research Council).

References

1. Shabestari SG, Moemeni H (2004) J Mater Process Technol 153 (4):193
2. Rooy EL (1988) Aluminum and aluminum alloys in castings: metals handbook, vol 15. ASM International, Metals Park, Ohio, USA, p 743
3. Heusler L, Schneider WG (2002) J Light Metals 2:17
4. Lozano JA, Peña BS (2006) Scripta Mater 54:943
5. Haque MM, Ismail AF (2005) J Mater Process Technol 162–163:312
6. Lu L, Nogita K, Dahle AK (2005) Mater Sci Eng A399:244
7. Gall K, Yang N, Horstemeyer M, McDowell DL, Fan J (2000) Fatigue Fract Eng Mater Struct 23:159
8. Han SW, Kim SW, Kumai S (2004) Fatigue Fract Eng Mater Struct 27:9
9. Petch NJ (1953) J Iron Steel Inst 174:25
10. Lasalmonie A, Strudel J (1986) J Mater Sci 21:1837
11. Kurzydlowski KJ, Ralph B, Bucki JJ, Garbacz A (1996) Mater Sci Eng A205:127
12. Dubé D, Couture A, Carbonneaut Y, Fiset M, Angers R, Tremblay R (1998) Int J Cast Met Res 11:139
13. Donelan P (2000) Mater Sci Technol 16:261
14. Osório WR, Garcia A (2002) Mater Sci Eng A325:103
15. Osório WR, Santos CA, Quaresma JMV, Garcia A (2003) J Mater Process Technol 143:703
16. Quaresma JMV, Santos CA, Garcia A (2000) Metall Mater Trans 31A:3167
17. Goulart PR, Spinelli JE, Osório WR, Garcia A (2006) Mater Sci Eng 421A:245
18. Osório WR, Freire CMA, Garcia A (2005) J Alloys Compd 397:179
19. Osório WR, Spinelli JE, Cheung N, Garcia A (2006) Mater Sci Eng 420A:179

20. Osório WR, Freire CMA, Garcia A (2005) J Mater Sci 40: 4493
21. Osório WR, Goulart PR, Moura Neto C, Garcia A (2006) Metall Mater Trans 37A:2525
22. Robles BP, Hernández A, Ortiz JI, Ortega R, Martínez EJ (2004) In: XIV Int Mater Res Cong, Cancún, México (August; CD-Rom)
23. Assis SL, Wolynec S, Costa I (2006) Electrochim Acta 51: 1815
24. Kliskic M, Radosevic J, Gudic S, Smith M (1998) Electrochim Acta 43:3241
25. Gudic S, Radosevic J, Kliskic M (2002) Electrochim Acta 47:3009
26. Osório WR, Siqueira CA, Freire CMA, Garcia A (2005) Rev Metalurgia Madrid Extr:176
27. Chalmers B (1964) Principles of solidification. Wiley, New York, p 30